Published in Journal of Electroanalytical Chemistry 581, issue 2, 265-274, 2005
which should be used for any reference to this work

Influence of cationic and anionic additives on the electrical properties of ionophore-based ion-selective membranes

Werner E. Morf [a,*], Nicolaas F. de Rooij [a], Ernö Pretsch [b]

[a] *Institute of Microtechnology (IMT), University of Neuchâtel, Rue Jaquet-Droz 1, CH-2007 Neuchâtel, Switzerland*
[b] *Laboratorium für Organische Chemie, Swiss Federal Institute of Technology (ETH-Hönggerberg), CH-8093 Zürich, Switzerland*

Abstract

The steady-state electrical behavior of cation-selective ionophore membranes with different kinds of ionic additives was studied on a theoretical basis. Membranes with both mobile and fixed anionic sites exhibit nonlinear current–voltage curves, which is in contrast with the ohmic behavior of pure fixed-site membranes. This can be explained from the specific concentration profiles in the membrane, illustrating pronounced polarization effects for the mobile sites. Surprisingly, the influence of the fixed sites on the current response is still observable even when the mobile sites predominate. At high voltages, current saturation occurs by limitations of the back-diffusion of free ionophores. This can be overcome when other, uncomplexed, cations contribute to the current flow. Membranes with both cationic and anionic sites cannot be strongly polarized, in analogy to other systems where an inert electrolyte is confined to a given phase. These membranes respond with current saturation at relatively low voltages. Currents above this limit can be achieved by an additional permeation of anions from the aqueous solution through the membrane, as shown by model calculations.

Keywords: Ion-selective electrodes; Solvent polymeric membranes; Current response; Theory; Steady-state; Concentration profiles

1. Introduction

Ionophore-based solvent polymeric membranes are widely used in ion-selective electrodes [1–7]. While potentiometry relies on so-called zero-current measurements, investigations with current polarization have a long-lasting tradition. Initially, they have been mainly applied for mechanistic studies [8–11]. More recently, various novel applications have been developed using external current for potentiometric measurements [12–14]. For example, zero-current ion fluxes have been compensated by an external current in order to improve the lower detection limit. Normal and pulsed galvanostatic measurements have been based on membranes without ion exchange properties [15–19]. Especially in the case of polyion sensing, they exhibit clear advantages as compared with traditional potentiometry [20]. Chronopotentiometry was demonstrated to be useful as a diagnostic tool to assess the concentration of active components in ion-selective membranes [21,22]. The current response of solvent polymeric membranes under controlled potential has been shown to be an equivalent choice to potentiometric determination of ion activities [23]. Experiments with current flow have also been used in spectroelectrochemical studies on ionophore-based ion-selective membranes [24].

In their simplest version, ionophore-based ISEs make use of membranes that consist of a 2:1 plasticizer-polymer phase with ~1 wt% of ionophore. It was shown earlier that such membranes apparently behave as phases with fixed anionic sites [3,8,25]. In fact, nearly all electrochemical and ion-selectivity characteristics of the

* Corresponding author. Tel.: +41 32 720 52 34; fax: +41 32 720 57 11.
E-mail address: werner.morf@unine.ch (W.E. Morf).

respective ISEs can be modeled perfectly on the basis of the appropriate fixed-site membrane theories [3,26–33] (for recent treatments, see [14,23,34–37]). It was suggested that the presence of anionic impurities originating from the fabrication of polymeric materials such as PVC is responsible for the observed effects [25,32,38].

Membranes with modified compositions have been introduced in order to vary the selectivity and the electrical properties of corresponding ISEs. The incorporation of lipophilic anions as mobile sites, in addition to the native fixed sites, was shown to increase the preference for divalent over monovalent cations, and to minimize the interference by sample anions, i.e., to improve the upper detection limits of the ISEs [3,39]. Further favorable effects reported include the efficient lowering of the membrane resistance, the reduction of the response time, and the improvement of the interfacial ion-exchange kinetics [40]. More recently, complete lipophilic salts have also been propagated as additives, which generate both cationic and anionic mobile sites in the membrane phase [41,42]. Such membrane modifiers were found to be beneficial for the respective sensors with regard to ion selectivity and membrane resistance [41,42].

Recently, we reported on a novel application of ionophore membrane electrodes as amperometric sensors [23,35]. The observed current responses at controlled potential were interpreted on the basis of a fixed-site membrane model, treating the membrane phase as an ohmic resistor with a given concentration of mobile cations. As a rule, the experimental data could be well fitted by the theoretical curves. However, membranes with added mobile anionic sites were also used in these studies, which were not adequately considered by the former treatment.

A series of theoretical models have been presented so far that can be applied, either directly [3,14,27,34,43,44] or after some extension, for the description of ISE membranes with incorporated mobile ions (for a review, see [3,4,36,45]). Most of these treatments were restricted to potentiometric systems at zero current, however. Actually, the basic problem for membranes with an amperometric current flow is that the mobile ionic sites, other than the fixed ones, tend to establish a concentration polarization [46,47]. The reason is that these species are driven by the applied electric field to one side of the membrane but, at the same time, they are strictly confined to the organic phase. Accordingly, the concentration profiles of ionic sites as well as of permeating ions may be completely different from the ones found at zero current. This implies that the electrical properties of the respective ISE systems also depend on the experimental parameters and may vary considerably between potentiometric and amperometric measurements.

An extended treatment of the steady-state and the transient current response of valinomycin-based membranes was offered by Nahir and Buck [47]. Using digital simulations, these authors studied the transport processes occurring in membranes that contain neutral ionophores, positive ion complexes, anionic sites, and ion pairs. They gave evidence for different processes controlling or limiting the current response (see also [21,48]). However, the treatments focused either on membranes with exclusively mobile sites [21,48] or on pure fixed-site membranes [32]. This is at variance with many real systems applied in routine analysis that incorporate different types of ionic sites. It will be shown that, surprisingly, fixed negative sites have a distinct influence on the current response of ionophore membranes, even when a 10-fold or higher excess of mobile anions exists in the organic phase. Another limitation of the earlier studies is their restriction to systems with only one permeating species. Accordingly, the analysis of data at very high voltages, where other ions apparently contribute to the current [8,27,47], is still an issue of speculation.

Here, we present a theoretical description of ionophore-based ISE membranes that contain any number of mobile anionic or cationic sites as well as fixed anionic sites. The mathematical model permits it to analyze the concentration profiles and the ion fluxes of all species in the membrane phase when an external voltage is applied that gives rise to a transmembrane current flow. For the sake of simplicity, the treatment is restricted to systems with singly charged ions and with relatively polar membrane media in which ion pair formation can be neglected. The basic results for concentration profiles and fluxes are derived from an extended steady-state solution of the transport equations.

2. Theory

The present treatment considers a membrane that contains permeating cations I^+ (as 1:n ion–ionophore complexes), any mobile ionic sites Q^+ and R^- trapped in the organic phase due to their lipophilicity, as well as fixed anionic sites S^-. At steady-state, the fluxes of these species are described by Eqs. (1)–(3):

$$J_\mathrm{i} = -D_\mathrm{i}\frac{\mathrm{d}C_\mathrm{i}}{\mathrm{d}x} - D_\mathrm{i}C_\mathrm{i}\frac{\mathrm{d}\psi}{\mathrm{d}x} = \mathrm{const}(x), \tag{1}$$

$$J_\mathrm{q} = -D_\mathrm{q}\frac{\mathrm{d}C_\mathrm{q}}{\mathrm{d}x} - D_\mathrm{q}C_\mathrm{q}\frac{\mathrm{d}\psi}{\mathrm{d}x} = 0, \tag{2}$$

$$J_\mathrm{r} = -D_\mathrm{r}\frac{\mathrm{d}C_\mathrm{r}}{\mathrm{d}x} + D_\mathrm{r}C_\mathrm{r}\frac{\mathrm{d}\psi}{\mathrm{d}x} = 0 \tag{3}$$

with:

$$\psi = \frac{F\phi}{RT}, \tag{4}$$

$$C_\mathrm{i}(x) + \sum C_\mathrm{q}(x) = \sum C_\mathrm{r}(x) + S_\mathrm{t}, \tag{5}$$

$$Q_\mathrm{t} = \frac{1}{d}\int_0^d \sum C_\mathrm{q}(x)\,\mathrm{d}x, \tag{6}$$

$$R_\mathrm{t} = \frac{1}{d}\int_0^d \sum C_\mathrm{r}(x)\,\mathrm{d}x, \tag{7}$$

where J is the flux, D the diffusion coefficient, and C the concentration of the subscripted species in the membrane, Ψ is a dimensionless potential function, ϕ is the local electrical potential, x is the coordinate in the membrane of thickness d ($0 \leqslant x \leqslant d$), S_t is the total concentration of fixed sites assumed to be invariant with x, Q_t and R_t are the average total concentrations of mobile cationic and anionic sites, respectively, F is the Faraday constant, R the universal gas constant, and T the absolute temperature. From Eqs. (2) and (3), a relationship between the steady-state distribution of mobile sites and the potential profile in the membrane is immediately found

$$\psi(x) - \psi(0) = -\ln\frac{\sum C_q(x)}{\sum C_q(0)} = \ln\frac{\sum C_r(x)}{\sum C_r(0)}. \tag{8}$$

From the sum $\sum J_v(D_i/D_v)$ for all species v, based on Eqs. (1), (2), (3) and (5), the flux of permeating cations can be expressed as

$$J_i = -D_i\left[2\frac{d(\sum C_r)}{dx} + S_t\frac{d\psi}{dx}\right] = \text{const}(x), \tag{9}$$

which leads to Eq. (10) where the definition $\Delta f = f(d) - f(0)$ is used for any function f:

$$J_i = -D_i\frac{2\Delta(\sum C_r) + S_t\Delta\psi}{d}, \tag{10}$$

$$\Delta\psi = \ln\frac{\sum C_r(d)}{\sum C_r(0)}. \tag{11}$$

Another expression for the flux is derived from Eq. (9) after multiplication with $\sum C_r$ and integration, making use of Eqs. (7) and (8):

$$J_i\sum C_r = -D_i\left[\frac{d(\sum C_r)^2}{dx} + S_t\frac{d(\sum C_r)}{dx}\right],$$

$$J_i = -D_i\frac{\sum C_r(d)(\sum C_r(d) + S_t) - \sum C_r(0)(\sum C_r(0) + S_t)}{R_t d}, \tag{12}$$

Eqs. (10)–(12) permit it to determine the boundary values $\sum C_r(0)$ and $\sum C_r(d)$ and the cation flux J_i as a function of $\Delta\Psi$:

$$\sum C_r(0) = \frac{0.5R_t}{e^{\Delta\psi}+1} \times\left[2 - \sigma + \sqrt{(2-\sigma)^2 + 4\sigma\Delta\psi\coth(0.5\Delta\psi)}\right], \tag{13}$$

$$\sum C_r(d) = \sum C_r(0)e^{\Delta\psi}, \tag{14}$$

$$J_i = -\frac{D_iR_t}{d}\left[\sigma\Delta\psi + \tanh(0.5\Delta\psi) \times\left\{2 - \sigma + \sqrt{(2-\sigma)^2 + 4\sigma\Delta\psi\coth(0.5\Delta\psi)}\right\}\right], \tag{15}$$

where $\sigma = S_t/R_t$ characterizes the ratio of fixed to mobile sites in the membrane.

Using the known boundary values, the complete concentration profile of sites R^- in the membrane can be described after integration of Eq. (9) from 0 to x, combination with Eq. (10), and substitution of the potential terms by Eq. (8)

$$2\sum C_r(x) + S_t\ln\sum C_r(x) = \left(1 - \frac{x}{d}\right)\left[2\sum C_r(0) + S_t\ln\sum C_r(0)\right] + \frac{x}{d}\left[2\sum C_r(d) + S_t\ln\sum C_r(d)\right]. \tag{16}$$

This implicit solution allows it to calculate the coordinate x for any value of $\sum C_r(x)$. The concentrations $\sum C_q(x)$ are then obtained, according to Eq. (8), as

$$\sum C_q(x) = \frac{P_{qr}}{\sum C_r(x)}, \tag{17}$$

where the concentration product P_{qr} is independent of x. The evaluation of this term requires multiplication of Eq. (9) with $\sum C_q$ and subsequent integration:

$$J_i\sum C_q = -D_iP_{qr}\left[2\frac{d\ln(\sum C_r)}{dx} - S_t\frac{d(\sum C_r)^{-1}}{dx}\right],$$

$$J_i = -D_iP_{qr}\frac{2\Delta\psi - S_t\Delta(1/\sum C_r)}{Q_t d}. \tag{18}$$

Hence, it follows with Eq. (10)

$$P_{qr} = Q_t\frac{2\Delta(\sum C_r) + S_t\Delta\psi}{2\Delta\psi - S_t\Delta(1/\sum C_r)}. \tag{19}$$

Finally, the concentration profile $C_i(x)$ of permeating cations is also determined

$$C_i(x) = \sum C_r(x) + S_t - \sum C_q(x). \tag{20}$$

The preceding treatment offers a straightforward modeling of ion concentrations and fluxes in a membrane that incorporates different types of ionic sites. However, the pivotal parameter entering in this description is the membrane-internal potential difference, $\Delta\phi = (RT/F)\Delta\Psi$, and not the transmembrane potential difference. The total membrane potential, $\Delta\phi_t$, which is the difference between the local potentials ϕ'_{aq} and ϕ''_{aq} in the aqueous solutions on both sides of the membrane, is composed of the membrane-internal contribution ($\Delta\Psi$, see Eq. (11)) and the difference of two boundary potential terms ($\Delta\Psi'_b - \Delta\Psi''_b$)

$$\Delta\phi_t = \phi''_{aq} - \phi'_{aq} = \frac{RT}{F}\left(\Delta\psi + \Delta\psi'_b - \Delta\psi''_b\right). \tag{21}$$

The additional potential difference is described by Morf et al. [3,14,34]

$$\Delta\Psi'_b - \Delta\Psi''_b = \ln\frac{a'_{i,aq}}{a''_{i,aq}} - \ln\frac{C_i(0)}{C_i(d)} + n\ln\frac{C_L(0)}{C_L(d)}, \quad (22)$$

where $a'_{i,aq}$ and $a''_{i,aq}$ are the activities of permeating ions in the two aqueous solutions, $C_i(0)$ and $C_i(d)$ are the concentrations of the 1:n ion–ionophore complexes at the two membrane boundaries, and $C_L(0)$ and $C_L(d)$ are the concentrations of free ionophores at the interfaces. For simplicity, it is assumed that the aqueous activities are high enough to be independent of ion fluxes [14,34], and that a symmetrical cell with $a'_{i,aq} = a''_{i,aq}$ is used. Hence, the total membrane potential difference becomes independent of the external activities. It should be pointed out that the validity and the applicability of the present theory do not hinge on the assumptions made with respect to the external solutions. To analyze specific situations such as the voltammetric interpretation of the potential at the aqueous/organic interface [10] or pulsed galvanostatic measurements [19,20], any other, for the specific case more appropriate description of the boundary potential difference can be chosen in place of Eq. (22). Such extensions are beyond the focus of the discussions given in this work, however.

The ion concentrations in Eq. (22) are given from the preceding procedure, whereas the ligand concentrations are obtained from the respective conservation law in the membrane at steady-state [3,27]:

$$C_{L,mean} = \frac{C_L(0) + C_L(d)}{2} = L_t - n(R_t + S_t - Q_t), \quad (23)$$

$$J_L = -D_L\frac{C_L(d) - C_L(0)}{d} = -nJ_i, \quad (24)$$

from which it follows:

$$C_L(0) = C_{L,mean} - J_i\frac{nd}{2D_L}, \quad (25)$$

$$C_L(d) = C_{L,mean} + J_i\frac{nd}{2D_L}. \quad (26)$$

Evidently, an iterative procedure is required for calculating the potential difference $\Delta\phi_t$ as a function of the current flow i through the membrane of area A.

$$i = FAJ_i. \quad (27)$$

3. Results and discussion

3.1. Membranes with lipophilic anions as additives

The electrochemical behavior of cation-selective membranes that incorporate both fixed and mobile anionic sites, but no cationic sites, is illustrated in Figs. 1–5. The calculations were based on the iterative procedure mentioned above. First, an initial value for the internal potential difference $\Delta\phi$ was chosen, and the

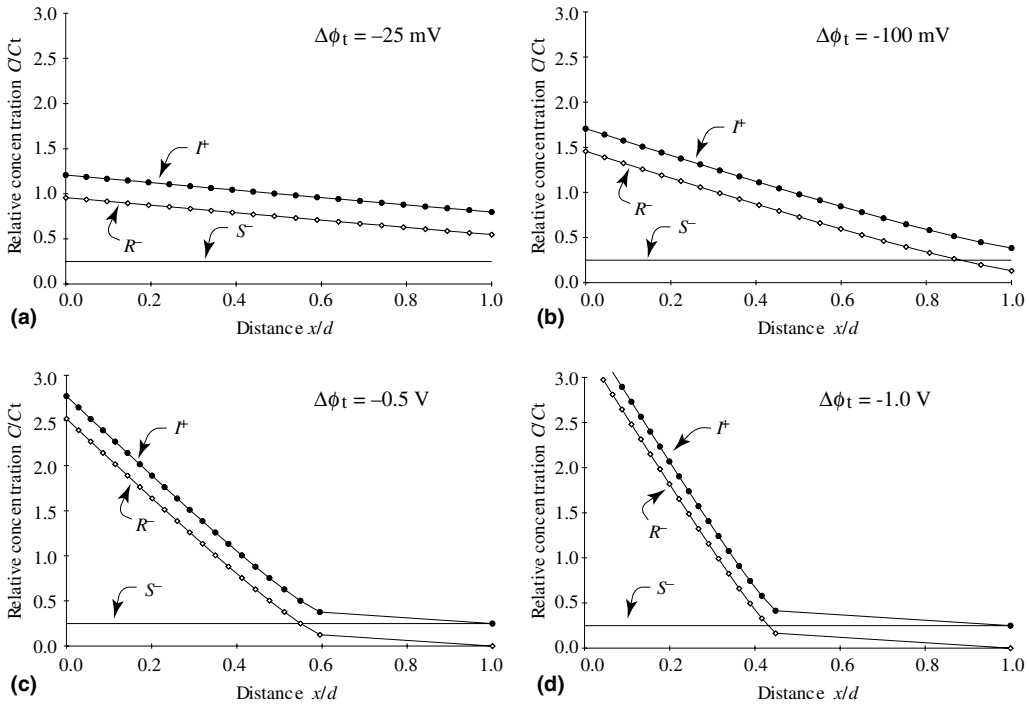

Fig. 1. Ion concentration profiles in a cation-selective ionophore membrane with anionic sites (ratio of fixed to mobile sites: $\sigma = 0.33$). The concentrations for I^+ (●), R^- (◇), and S^- (—) are given as fractions of the average total ion concentration C_t. The applied potential differences are −25 mV (a), −100 mV (b), −0.5 V (c), and −1 V (d). The resulting currents for (b), (c), and (d) are 3.4, 9.7 and 16.3 times higher than for (a), respectively.

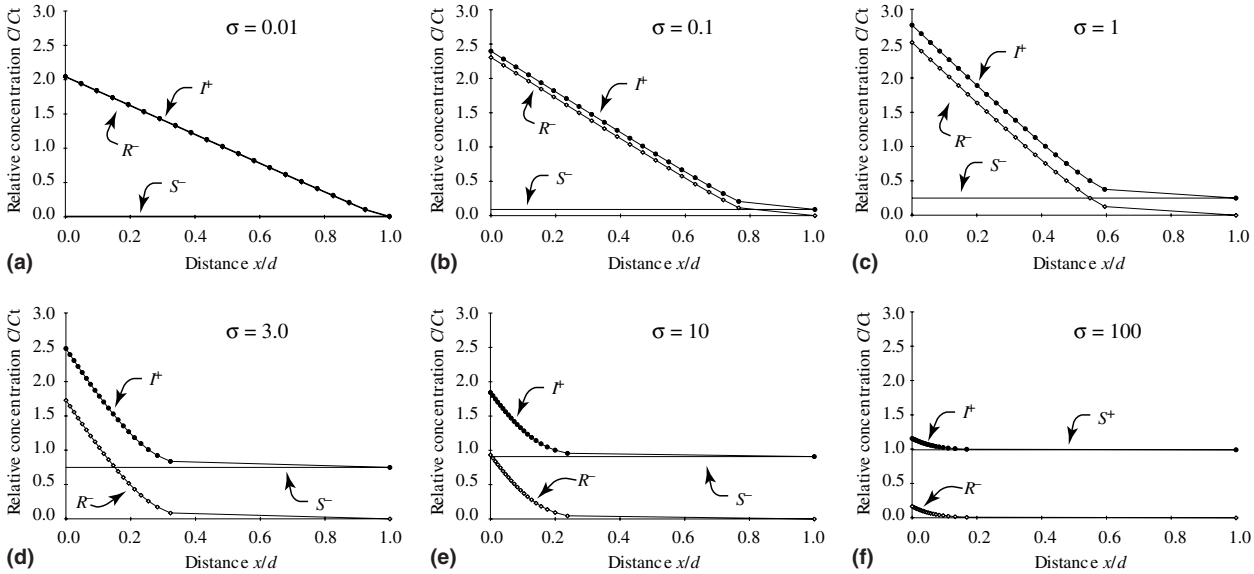

Fig. 2. Ion concentration profiles in membranes with different ratios σ of fixed to mobile sites. Concentrations at a potential difference of −0.5 V are shown for $\sigma = 0.01$ (a), 0.1 (b), 1 (c), 3 (d), 10 (e), and 100 (f), respectively. More details as well as the solution for $\sigma = 0.33$ are given in Fig. 1.

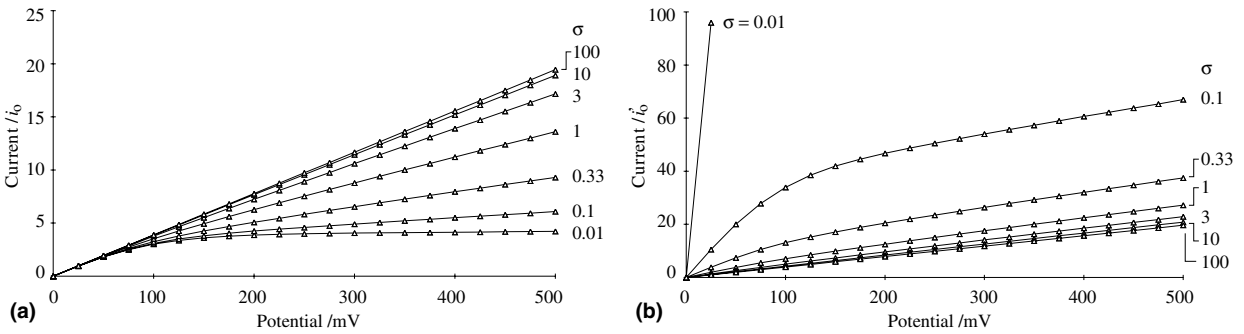

Fig. 3. Current–voltage curves for cation-selective ionophore membranes with fixed and mobile anionic sites (ratio σ). (a) Currents in units of $i_o = FAD_iC_t/d$ for membranes with the same C_t and with $\sigma = 0.01$, 0.1, 0.33, 1, 3, 10, 100, respectively (curves from bottom to top). (b) Currents in units of $i'_o = FAD_iS_t/d$ for membranes with the same S_t and with $\sigma = 0.01$, 0.1, 0.33, 1, 3, 10, 100, respectively (curves from top to bottom).

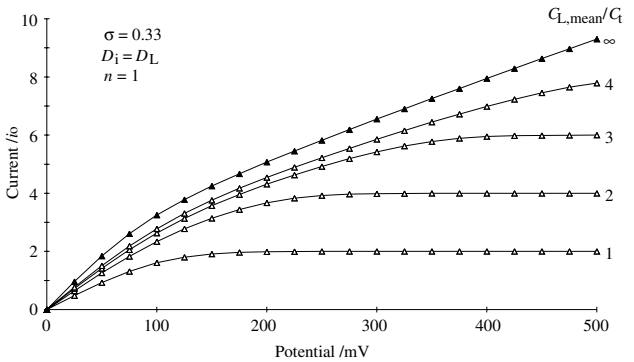

Fig. 4. Influence of the ionophore concentration on the current–voltage curve of membranes with fixed and mobile anionic sites (ratio $\sigma = 0.33$). The curves were calculated for $n = 1$ and $D_i = D_L$ and refer to membranes with $C_{L,mean}/C_t = 1$, 2, 3, 4, and ∞, respectively (curves from bottom to top). The curve with dark symbols corresponds to the respective one in Fig. 3.

respective concentration profiles were evaluated. Then, the corresponding boundary potential term $\Delta\phi'_b - \Delta\phi''_b$ and the total membrane potential $\Delta\phi_t$ were determined. A comparison with the true value $\Delta\phi_t$ led to the next approximation for $\Delta\phi$, and so forth. The calculations were performed with conventional MS Excel software (Microsoft Corporation). For simplicity, it was assumed for Figs. 1–3 that the membrane phase contains a large excess of free ionophores, so that the approximation $C_L(0) = C_L(d) = C_{L,mean}$ can be used in Eq. (22).

Fig. 1 shows the concentration profiles of permeating cations and anionic sites in a membrane for which the ratio of fixed to mobile sites is $\sigma = 0.33$. The influence of the applied potential and of the resulting current flow, respectively, is demonstrated. Evidently, the electrodialytic cation transport is always accompanied by a concentration polarization of mobile sites in the membrane. Generally, an enrichment of the trapped anions on the

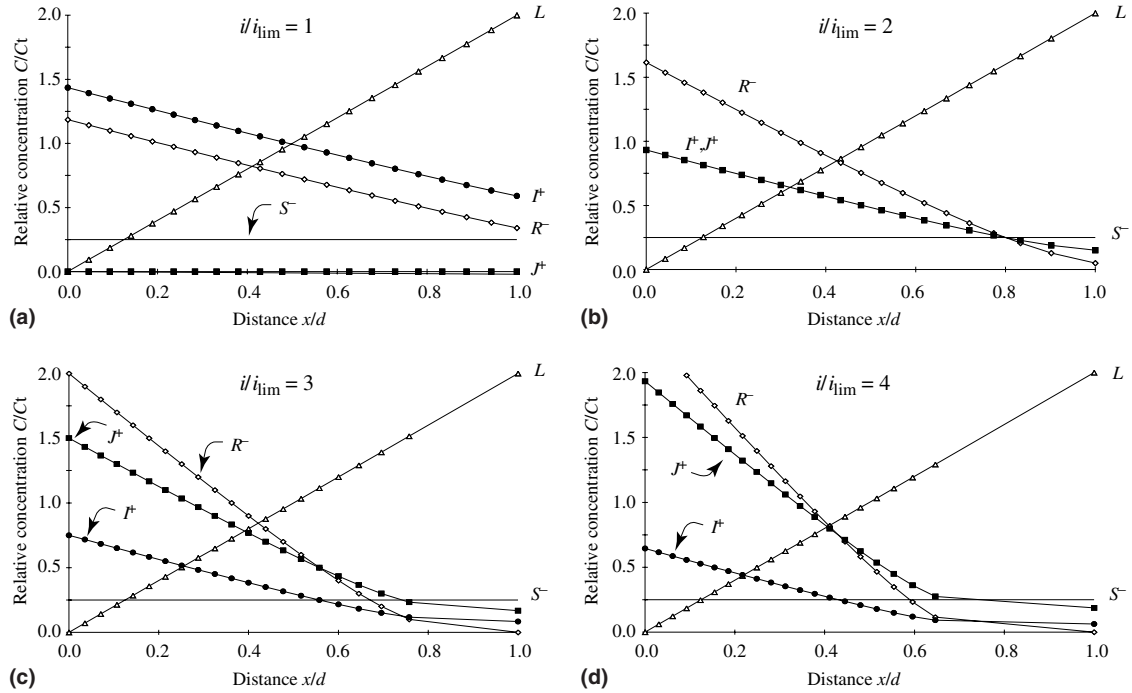

Fig. 5. Concentration profiles for cationic species, anionic sites, and free ionophores in a membrane with $\sigma = 0.33$ and $C_{L,mean} = C_t$ at very high voltages and currents, respectively. The concentrations for I^+ (●, complexed), J^+ (■, uncomplexed), R^- (◇), S^- (—), and L (△) are given as fractions of the average total ion concentration C_t. Calculations using the assumption $D_i = D_j$ were performed for currents of $i/i_{lim} = 1$ (a), 2 (b), 3 (c), and 4 (d), respectively, where i_{lim} is the limiting current reached in the absence of J^+ (Fig. 4). The curves for I^+ and J^+ coincide in case (b).

side where the cations enter the membrane, and their depletion on the opposite side, is observed. The extent of these effects depends on the applied voltage since the concentration gradient of mobile sites is built up as a driving force that compensates the oppositely directed force by the electric field. Very surprisingly, the concentration profiles established at -0.5 and -1 V are quite different from the perfectly linear profiles found in the absence of fixed sites [46]. The present results suggest that the electric conductance at high voltages will rather reflect the fixed-site concentration in the membrane, but will be determined by the sum of fixed and mobile sites near zero current (see also below).

Fig. 2 illustrates calculated results for membranes that differ in the fixed to mobile site ratio σ. In this case, a given total potential difference of -0.5 V was applied. The plotted concentration profiles document a nearly constant gradient of ionic species within a membrane with $\sigma \ll 1$, which agrees with the findings reported earlier for pure liquid ion-exchanger membranes [46]. In contrast, if $\sigma \gg 1$ holds, the mobile sites are strongly enriched near one boundary so that the main part of the membrane is fully dominated by the fixed sites.

Fig. 3(a) shows current–voltage curves for membranes that have a given total concentration $C_t = R_t + S_t$ of anionic sites at varying ratios σ. The calculated currents are given in arbitrary units, defined as $i_o = FAD_iC_t/d$. Again, the cases of a low and a high ratio of fixed to mobile sites can be discerned. For $\sigma \ll 1$, the plots are clearly curved and indicate a near current saturation at higher voltages. This behavior conforms to the findings in Fig. 2(a) where the cation flux is obviously limited by the maximum attainable gradient of ion concentration in the membrane. For $\sigma \gg 1$, on the other hand, the current–voltage plots are nearly linear and in accord with the expected ohmic behavior of a pure fixed-site membrane. Such characteristics were indeed observed for cation-selective ionophore membranes without mobile anionic additives [3,8,26]. It should be noted that the curve for $\sigma = 100$ in Fig. 3(a) can be perfectly identified with the response found for a pure fixed-site membrane ($\sigma \to \infty$), the relative deviations being <0.1% throughout. In contrast, the curves for $\sigma = 0.1$ or $\sigma = 0.01$ turn out to diverge from the response obtained for a membrane without any fixed sites ($\sigma = 0$). The deviations calculated for the two curves at -0.5 V are as high as 52% and 6%, respectively. Evidently, fixed negative sites still have a distinct influence on the electrical properties of ionophore-based membranes, even when a 10- to 100-fold excess of mobile anions is added. This effect is unexpectedly high, especially when Fig. 2(a) is considered where the concentration profiles approximate the ideally linear traces for membranes without fixed sites.

A different view is presented in Fig. 3(b) where current data in units $i'_o = FAD_iS_t/d$ are given for

membranes with a constant concentration S_t of fixed sites and varying amounts of mobile sites. The results are in accord with experimental evidence on cation-selective ionophore membranes that the addition of anionic additives generally increases the electric conductivity. Surprisingly, the slopes of the curves at higher voltages turn out to be almost identical, which nicely corroborates the uniform effect of the fixed-site population on the membrane conductance. These results clearly demonstrate that the electrical influence of fixed negative sites in membranes with mobile anionic additives cannot be neglected, even when the concentration of mobile sites is 10–100 times higher than the fixed-site content. In common plasticized PVC membranes, as used for ion-selective electrode applications, the total concentration of anionic impurities behaving as fixed sites was determined to be between 0.07 and 0.8 mmol kg^{-1} [25,49–53]. Thus, the predicted influence of fixed sites would be observable up to around 100 mmol kg^{-1} of mobile sites. This is far above the usually applied amounts of mobile sites in ISE membranes (1–10 mmol kg^{-1}) [4].

Fig. 3(b) also offers some insight into the expected amperometric response behavior of membranes with both fixed and mobile anionic sites. Actually, if a gradient of the external cation activities would be applied as the driving force, instead of the electrical potential difference, the resulting traces of the current response vs. $\log(ai'/ai'')$ would be qualitatively the same as in Fig. 3(b). It can be concluded that the addition of large amounts of mobile sites leads to considerably higher slopes of the amperometric response but, on the other hand, also to pronounced nonlinearities. In contrast, small amounts of additives do not alter the response characteristics seriously. Further influences on the amperometric response behavior were discussed earlier [14,23].

Fig. 4 shows the influence of the free ionophore concentration on the electric properties of the membrane. With decreasing $C_{L,mean}$, the accessible concentration gradient for the back diffusion of free ligands is reduced, which also sets a limit to the carrier-mediated ion flux at steady-state. Finally, a limiting current is dictated which, according to Eqs. (25)–(27), is given by $i_{lim} = 2FAD_L C_{L,mean}/nd$. The curves in Fig. 4 illustrate that this saturation current is strictly proportional to the available concentration of free ionophores. Another interesting observation is that, even at low voltages, there is a clear gap between the curves calculated for finite and infinite ionophore concentrations, respectively. The difference between two curves at a given current level can be identified with the respective boundary potential difference, which depends on the actual values of the boundary concentrations, $C_L(0)$ and $C_L(d)$.

Current values above i_{lim} may be established at very high voltages for which the condition $C_L(0) \to 0$ is approximated. In this case, a major part of the applied potential drop acts at the interface where cations enter the membrane. Due to the modified extraction properties at $x = 0$, the membrane may also become permeable for other, uncomplexed, cations. Experimental evidence for such current enhancements was given earlier but the basic mechanisms could not be explained cogently [8,47,48]. The exact situation is documented in Fig. 5 where concentration profiles for the primary ion and a new species are depicted. For these calculations, the present model had to be extended to account for different permeating cations. The full details of such procedures can be found in the literature [3,14,34] and will not be recapitulated here.

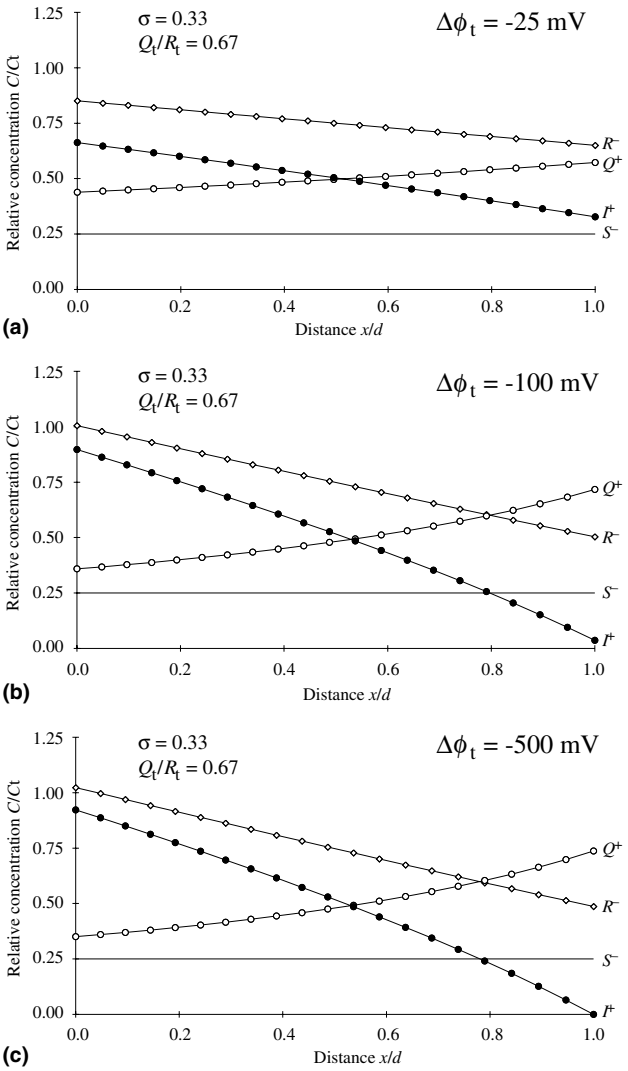

Fig. 6. Ion concentration profiles in a cation-selective ionophore membrane with both cationic and anionic sites ($\sigma = 0.33$, $Q_t/R_t = 0.67$). The concentrations for I^+ (●), Q^+ (○), R^- (◇), and S^- (—) are given as fractions of the average total ion concentration C_t. The potential differences are −25 mV (a), −100 mV (b), and −0.5 V (c); the currents for (b) and (c) are 2.5 and 2.7 times higher than for (a), respectively.

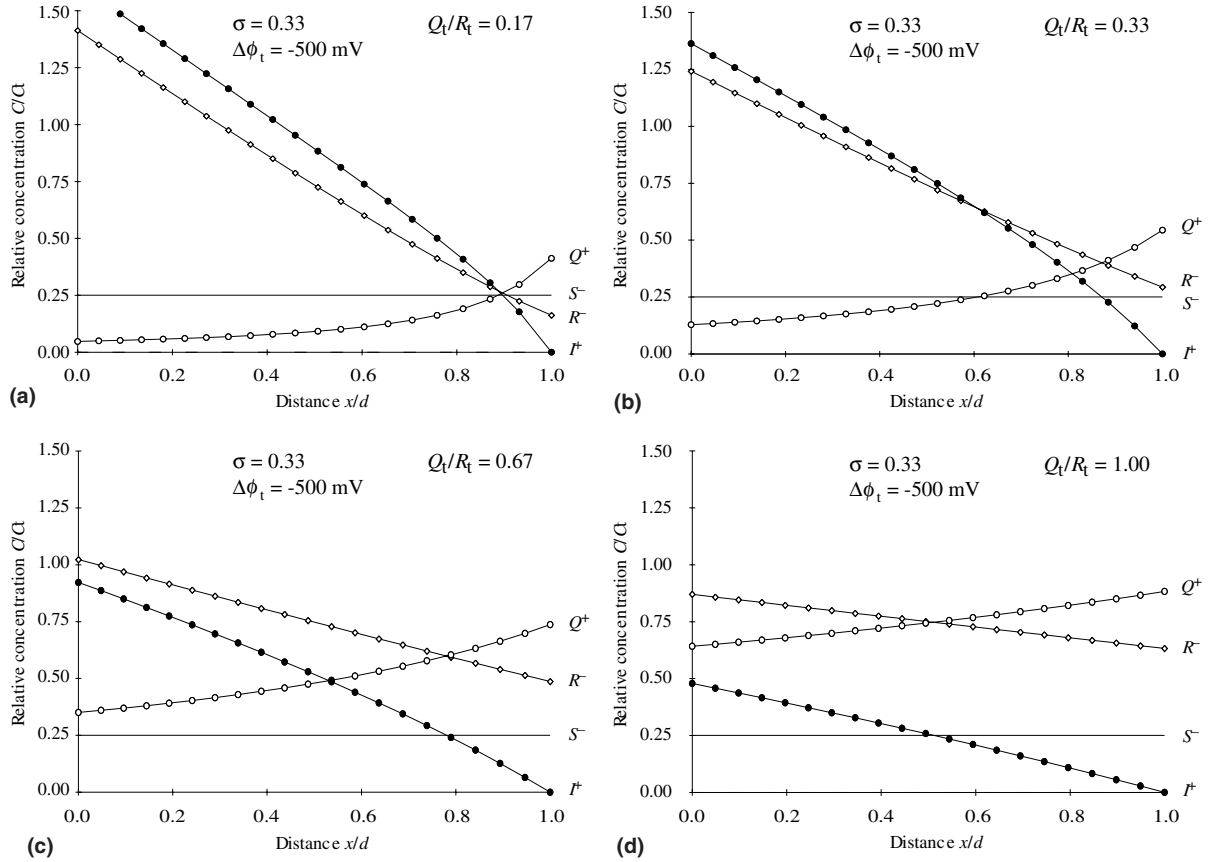

Fig. 7. Ion concentration profiles in membranes with $\sigma = 0.33$ and $Q_t/R_t = 0.17$ (a), 0.33 (b), 0.67 (c), and 1 (d), respectively, at a potential difference of −0.5 V. See Fig. 6 for additional details.

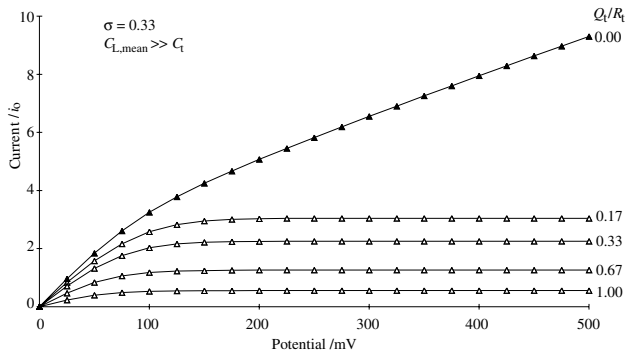

Fig. 8. Current–voltage curves for cation-selective ionophore membranes with cationic and anionic sites ($\sigma = 0.33$). The currents are given in units of $i_o = FAD_iC_t/d$ for membranes with $Q_t/R_t = 0$, 0.17, 0.33, 0.67, and 1, respectively (curves from top to bottom). The curve with dark symbols refers to Fig. 4.

3.2. Membranes with salts, consisting of lipophilic cations and anions, as additives

The electrochemical behavior of cation-selective ionophore membranes with fixed and mobile anionic sites as well as mobile cationic sites is characterized in Figs. 6–9. The basic calculations relied on the preceding treatment where, as in Figs. 1–3, the simplifying assumption $C_{L,mean} \gg C_t$ was used.

Fig. 6 illustrates the distribution of all ionic species within a given membrane at different values of the applied voltage. Obviously, the influence of the electric field leads to a certain movement of mobile anionic and cationic sites in different directions. However, in contrast to the former case, this concentration polarization is clearly limited since the condition of electroneutrality does not permit larger separations of positive and negative sites. Such behavior is comparable to that of solutions with inert background electrolytes, as used in classical electroanalysis. The observed effects in Fig. 6 are therefore much less pronounced than for the same system without cationic membrane components (Fig. 1). Actually, in the present case, only a minor fraction of the total potential difference can be applied within the interior of the membrane. A major part of the voltage usually drops at the interface where the cations leave the membrane. This is quite obvious at voltages of $-\Delta\phi_t > 0.1$ V where the system approaches a limiting state with $C_i(d) \to 0$ (see Fig. 6(c) and Eq. (22)). The results suggest that membranes of this type generally exhibit a current saturation at relatively low voltages.

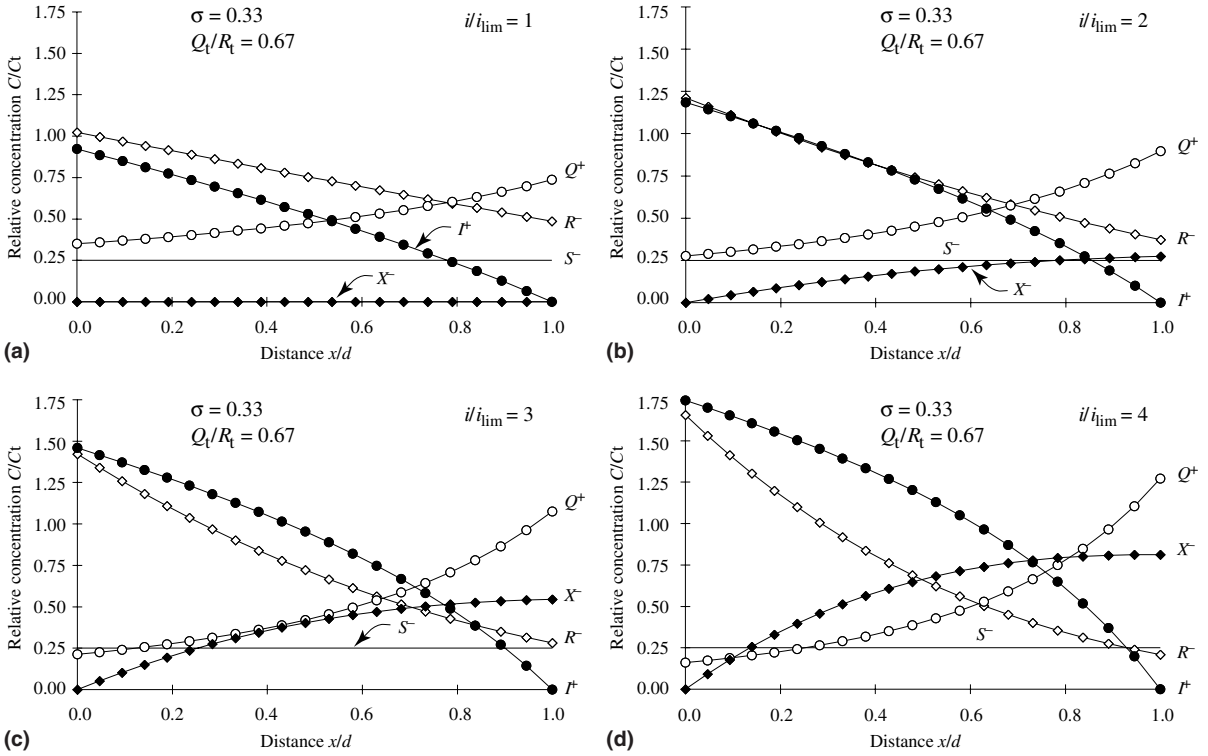

Fig. 9. Concentration profiles for permeating cations and anions (dark symbols) and for cationic and anionic sites in a membrane with $\sigma = 0.33$ and $Q_t/R_t = 0.67$ at very high voltages. The concentrations for I^+ (●), X^- (◆), Q^+ (○), R^- (◇), and S^- (—) are given in units of $C_t = R_t + S_t$. Calculations using the assumption $D_i = D_x$ were performed for currents of $i/i_{lim} = 1$ (a), 2 (b), 3 (c), and 4 (d), respectively, where i_{lim} is the limiting current in the absence of X^- (Fig. 8).

Fig. 7 illustrates the distribution of ionic species in membranes with varying amounts of positively charged additives at the same potential difference of −0.5 V. The higher the concentration of cationic sites is, the lower are the relative shifts of mobile sites induced by the electric field. The shown concentration profiles clearly indicate that a limiting state is reached in all cases, since the concentration of permeating ions at the boundary $x = d$ is always near zero. Hence, all these systems should respond with a limiting current at moderate voltages.

Fig. 8 shows the full current–voltage characteristics of the membranes studied before. The displayed curves are actually of the saturation type, as predicted above. The limiting currents are found to decrease with increasing amounts of cationic additives. Two reasons are responsible for this behavior: first, the lower concentration of permeating ions in the presence of cationic additives and, second, the lower extent of polarization realized in such membranes.

Again, the limiting currents established for systems with only one permeating species may be exceeded as soon as additional permeants contribute to the transmembrane flow of charge. At very high voltages, an extraction of sample anions at the membrane boundary at $x = d$ is here strongly favored by both the presence of cationic sites and by the large interfacial potential difference acting in such cases. This situation turns out to be different from the findings for membranes without positively charged sites where additional cationic permeants were involved in the current increase. Fig. 9 provides some information on the concentration profiles of permeating cations and anions at currents above the respective limiting values established in Fig. 8. For these calculations, an extended version of Schlögl's treatment [3,54] of fixed-site membranes with several ion classes was developed and applied. To be brief, no details of the corresponding lengthy procedures will be submitted. The results in Fig. 9 clearly demonstrate that an increasing extraction of anions is required to increase the accessible current values beyond the limits dictated for a purely cation-permeable membrane system.

4. Conclusions

The electrical behavior of ionophore-based membranes with different kinds of ionic sites was studied on the basis of an extended theoretical treatment. It was shown that membranes with both mobile and fixed anionic sites are characterized by nonlinear current–voltage curves. This was explained by polarization effects arising in the case of mobile sites, and was illustrated by concentration profiles calculated for the membrane phase. It

was documented, however, that the influence of fixed sites cannot be completely neglected even in cases where the mobile sites predominate. On the other hand, a current saturation was generally observed at high voltages, originating from limitations of the free ionophore transport. Currents exceeding this limit can be realized by a co-permeation of other, uncomplexed cations.

Membranes with anionic as well as cationic sites were found to respond with current saturation at relatively low voltages. It was demonstrated by computed ion profiles that such phases with trapped electrolytes are only moderately polarizable. This behavior is analogous to the one of polarographic systems where inert background electrolytes are used to minimize polarization effects in the aqueous phase. To achieve current values above the saturation level, the additional permeation of anions from the aqueous solution through the membrane was proven to be a possible mechanism in the present case.

Acknowledgments

The authors thank the Swiss National Science Foundation and the National Institutes of Health (Grant R01-EB002189) for financial support.

References

[1] J. Koryta, K. Stulik, Ion-selective Electrodes, second ed., Cambridge University Press, Cambridge, GB, 1983.
[2] H. FreiserIon-selective Electrodes in Analytical Chemistry, vol. 1, Plenum Press, New York, 1978.
[3] W.E. Morf, The Principles of Ion-selective Electrodes and of Membrane Transport, Elsevier, New York, 1981.
[4] E. Bakker, P. Bühlmann, E. Pretsch, Chem. Rev. 97 (1997) 3083.
[5] P. Bühlmann, E. Pretsch, E. Bakker, Chem. Rev. 98 (1998) 1593.
[6] E. Bakker, P. Bühlmann, E. Pretsch, Electroanalysis 11 (1999) 915.
[7] R.P. Buck, E. Lindner, Anal. Chem. 73 (2001) 88A.
[8] A.P. Thoma, A. Viviani-Nauer, S. Arvanitis, W.E. Morf, W. Simon, Anal. Chem. 49 (1977) 1567.
[9] T. Kakiuchi, M. Senda, Bull. Chem. Soc. Jpn. 57 (1984) 1801.
[10] S. Kihara, Z. Yoshida, Talanta 31 (1984) 789.
[11] Y. Yoshida, M. Matsui, K. Maeda, S. Kihara, Anal. Chim. Acta 374 (1998) 269.
[12] E. Lindner, R.E. Gyurcsányi, R.P. Buck, Electroanalysis 11 (1999) 695.
[13] E. Pergel, R.E. Gyurcsányi, K. Tóth, E. Lindner, Anal. Chem. 73 (2001) 4249.
[14] W.E. Morf, M. Badertscher, T. Zwickl, N.F. de Rooij, E. Pretsch, J. Electroanal. Chem. 526 (2002) 19.
[15] V. Horváth, G. Horvai, E. Pungor, Mikrochim. Acta 1990 (I) (1990) 217.
[16] H.J. Lee, P.D. Beattie, B.J. Murray, D. Osborne, H.H. Girault, J. Electroanal. Chem. 440 (1997) 73.
[17] S. Jadhav, A.J. Meir, E. Bakker, Electroanalysis 12 (2000) 1251.
[18] S. Makarychev-Mikhailov, A. Shvarev, E. Bakker, J. Am. Chem. Soc. 126 (2004) 10548.
[19] A. Shvarev, E. Bakker, Anal. Chem. 75 (2003) 4541.
[20] A. Shvarev, E. Bakker, J. Am. Chem. Soc. 125 (2003) 11192.
[21] B.D. Pendley, R.E. Gyurcsányi, R.P. Buck, E. Lindner, Anal. Chem. 73 (2001) 4599.
[22] B.D. Pendley, E. Lindner, Anal. Chem. 71 (1999) 3673.
[23] J. Sutter, W.E. Morf, N.F. de Rooij, E. Pretsch, J. Electroanal. Chem. 571 (2004) 27.
[24] R.E. Gyurcsányi, E. Lindner, Anal. Chem. 77 (2005) 2132.
[25] W.E. Morf, W. Simon, Helv. Chim. Acta 69 (1986) 1120.
[26] W.E. Morf, P. Wuhrmann, W. Simon, Anal. Chem. 48 (1976) 1031.
[27] W.E. Morf, L.F.J. Dürselen, W. Simon, in: E. Roth (Ed.), Reviews on Analytical Chemistry, Les Éditions de Physique, Les Ulis Cedex: France, 1988, p. 271.
[28] P.C. Meier, W.E. Morf, M. Läubli, W. Simon, Anal. Chim. Acta 156 (1984) 1.
[29] E. Bakker, R.K. Meruva, E. Pretsch, M.E. Meyerhoff, Anal. Chem. 66 (1994) 3021.
[30] M. Nägele, E. Bakker, E. Pretsch, Anal. Chem. 71 (1999) 1041.
[31] R.P. Buck, in: H. Freiser (Ed.), Ion-selective Electrodes in Analytical Chemistry, vol. 1, Plenum Press, New York, 1978, p. 1.
[32] T.M. Nahir, R.P. Buck, J. Electroanal. Chem. 341 (1992) 1.
[33] T. Kakiuchi, Anal. Chem. 68 (1996) 3658.
[34] W.E. Morf, M. Badertscher, T. Zwickl, N.F. de Rooij, E. Pretsch, J. Phys. Chem. B 103 (1999) 11346.
[35] W.E. Morf, T. Zwickl, E. Pretsch, N.F. de Rooij, Chimia 57 (2003) 639.
[36] E. Bakker, P. Bühlmann, E. Pretsch, Talanta 63 (2004) 3.
[37] A. Radu, A.J. Meir, E. Bakker, Anal. Chem. 76 (2004) 6402.
[38] A. van der Berg, P.D. van der Waal, M. Skowronska-Ptasinska, E.J.R. Sudhölter, D.N. Reinhoudt, P. Bergveld, Anal. Chem. 58 (1987) 2827.
[39] R. Eugster, P.M. Gehrig, W.E. Morf, U.E. Spichiger, W. Simon, Anal. Chem. 63 (1991) 2285.
[40] P. Gehrig, W.E. Morf, M. Welti, E. Pretsch, W. Simon, Helv. Chim. Acta 73 (1990) 203.
[41] D. Ammann, E. Pretsch, W. Simon, E. Lindner, A. Bezegh, E. Pungor, Anal. Chim. Acta 171 (1985) 119.
[42] M. Nägele, Y. Mi, E. Bakker, E. Pretsch, Anal. Chem. 70 (1998) 1686.
[43] W.E. Morf, W. Simon, Anal. Lett. 22 (1989) 1171.
[44] A. Ceresa, A. Radu, S. Peper, E. Bakker, E. Pretsch, Anal. Chem. 74 (2002) 4027.
[45] E. Bakker, D. Diamond, A. Lewenstam, E. Pretsch, Anal. Chim. Acta 393 (1999) 11.
[46] J.R. Sandifer, R.P. Buck, J. Phys. Chem. (1975) 384.
[47] T.M. Nahir, R.P. Buck, J. Phys. Chem. 97 (1993) 12363.
[48] T.M. Nahir, R.P. Buck, Talanta 41 (1994) 335.
[49] Y. Qin, E. Bakker, Anal. Chem. 73 (2001) 4262.
[50] E. Lindner, E. Gráf, Z. Nigreisz, K. Tóth, E. Pungor, R.P. Buck, Anal. Chem. 60 (1988) 295.
[51] M. Nägele, E. Pretsch, Mikrochim. Acta 121 (1995) 269.
[52] P. Bühlmann, S. Yajima, K. Tohda, K. Umezawa, S. Nishizawa, Y. Umezawa, Electroanalysis 7 (1995) 811.
[53] R.E. Gyurcsányi, E. Lindner, Anal. Chem. 74 (2002) 4060.
[54] R. Schlögl, Ber. Bunsenges. Phys. Chem. 82 (1978) 225.